is evident from the values of Θ_0 listed in the table, the amplitude of the motion at the β and γ positions is substantially larger than that at the δ position.

Inversion-recovery spectra of $^2H_6$-Pro, observed at 20 °C, were in good agreement with spectra calculated by using eq 9 together with the values of Θ_0 and ν_Q for each ring position, Table III, measured from the $^2H_6$-Pro line shape. The same correlation time, 1.1 ps, was used for all three ring positions to calculate the inversion-recovery spectra and was in close agreement with the correlation time observed for $^2H_2$-Pro, Table II. The correlation time obtained for $^2H_6$-Pro·HCl, 0.3 ps, is also in agreement with that listed for $^2H_2$-Pro·HCl in Table II. It is noteworthy that, in spite of the large T_1 values predicted and observed for the hydrochloride compounds, spin diffusion did not cause the angular dependence of T_1 to deviate significantly from that predicted by eq 9.

It is interesting to compare the values of Θ_0 in Table III with the values of Θ_0 obtained from London's analysis[16] of proline ^{13}C NT_1 values measured for peptides in solution. From London's Table I, one finds that Θ_0 is ca. 25° for β and γ positions and is about half as large for the δ position.[36] These results are in close agreement with results in Table III, especially when one considers the obvious difference in ring environments in the two cases. The similarity in Θ_0 values probably arises for the following reasons: First, the peptide nitrogen and α carbon are nearly immobilized by hydrogen bonds in the crystal; in solution these atoms have highly restricted internal motions because they are part of the peptide backbone. Second, the proline ring in the crystal structure[7] resides in a hydrophobic layer which evidently allows as much motional freedom as exists in solution.

In London's analysis,[16] the correlation time for the ring motion was not obtained since analysis of solution relaxation parameters yields the order parameter (amplitude) but not the rate of a very fast internal motion.[37] London did find that $\tau_e < 10^{-10}$ s was required to fit the relaxation data in solution. This result is fully in agreement with the results found herein.

The crystal structure of DL-Pro·HCl shows that the proline ring has an unusual average structure in which the ring is puckered (exo) at the α carbon with the four remaining ring atoms nearly coplanar. In addition the principal axes of the thermal ellipsoids suggest that the β, γ, and δ carbons undergo large amplitude motions in a direction perpendicular to the average plane formed by the nitrogen-C(3)-C(4)-C(5) atoms.

The NMR data show that the large thermal factors do indeed result from such motions rather than from a static statistical distribution of ring structures. Because of the unusual ring puckering and the difference in motional amplitude of the β and δ carbons, it is difficult to describe the ring motion in terms of a simple model. However, it may be possible to simulate the complex motion of the proline ring by means of a molecular mechanics calculation.[38] Indeed, DL-Pro·HCl is an ideal test case for such calculations because its crystal structure is known, and the motions involved are on the picosecond time scale.

A survey of over 50 crystal structures of imino acid and peptide derivatives of proline[5] has shown that the observed ring conformations are consistent with torsional potentials about single bonds. The particular ring conformations found in a specific case are usually determined by packing constraints within the crystal lattice. In the case of DL-proline and its hydrochloride, the proline rings appear to have about as much freedom to move as in solution. The exception to this statement occurs below -85 °C, for $^2H_2$-Pro, where we have suggested that contraction of the crystalline lattice restricts the amplitude of the ring motion. Contraction of the myoglobin unit cell volume has been observed at low temperature.[39] Measurements of the crystal structure of $^2H_2$-Pro in the -80 to -180 °C temperature range would be most interesting, because one could correlate the observed changes in ring dynamics with changes in intermolecular interactions and packing. The different dynamic behavior of the two proline rings in crystalline *cyclo*-(Gly-Pro-D-Ala)$_2$ has demonstrated the sensitivity of proline ring dynamics to molecular environment.[9]

The sensitivity of proline ring dynamics to intermolecular interactions suggests that proline relaxation measurements should be a useful probe of molecular packing within proteins. Such experiments will require enrichment with labeled proline residues but should be worth the effort since they have the potential to provide information about the fluidity of the protein interior in the neighborhood of each proline ring. In addition, one can monitor the influence of interesting variables such as pressure, ligand binding, and temperature on the proline ring environment.

Acknowledgment. We have benefited from helpful discussions with Dr. Attila Szabo, and we thank C. E. Sullivan and R. G. Tschudin for expert technical support.

(36) The equation relating Θ_0 to London's[16] angles β and θ is $\cos 2\Theta_0 = \cos^2\beta + \sin^2\beta \cos 2\theta$.

(37) Lipari, G.; Szabo, A. *J. Am. Chem. Soc.* **1982**, *104*, 4546-4559.

(38) Karplus, M.; McCammon, J. A. *CRC Crit. Rev. Biochem.* **1981**, *9*, 293-349.

(39) Petsko, G. A.; Ringe, D. *Annu. Rev. Biophys. Bioeng.* **1984**, *13*, 331-371.

Low-Temperature Carbon-13 Magnetic Resonance in Solids. 7. Methyl Carbons†

Mark S. Solum, Julio C. Facelli, Josef Michl, and David M. Grant*

Contribution from the Department of Chemistry, University of Utah, Salt Lake City, Utah 84112. *Received February 18, 1986*

Abstract: The principal values of the ^{13}C shielding tensors for a variety of methyl groups in small organic molecules are reported at 25 K. They were measured on neat samples of natural abundance materials. The assignment of the experimental principal values of the shielding tensors to the molecular frame was based on ab initio IGLO (Individual Gauge for Localized Orbitals) calculations of the shielding tensor for cases not determined by symmetry. The analysis of the IGLO bond contributions in the local bond frame was used to obtain some insight into the origin of the chemical shielding and, particularly, of the small variation of the σ_{33} component from compound to compound.

I. Introduction

Recently the use of low-temperature ^{13}C NMR spectroscopy combined with quantum mechanical calculations has been found very useful in the assignment of chemical shielding tensor components with the attendant elucidation of electronic structural features important in nuclear shielding in small organic molecules. Previous work from this laboratory reported the ^{13}C shielding tensors of methylene carbons in a large variety of compounds,[1]

† Part 6 of this series: ref 2.

0002-7863/86/1508-6464$01.50/0

of some methine carbons,[2] of a series of alkenes and cycloalkenes,[3] of some linear and pseudolinear molecules,[4] and of cyclopropane, bicyclo[1.1.0]butane, and [1.1.1]propellane.[5] In this paper a variety of methyl and methoxy ^{13}C shielding tensors are reported. The experimental tensor components were determined from a least-squares fitting of the experimental spectrum. The procedure uses a simplex algorithm and the new integration technique POWDER.[6] Possible intermolecular effects on the shielding tensor in methanol are also discussed.

Since all the shielding tensors reported here were measured on powder samples, the orientation of the tensors was not determined experimentally, but it was derived from Individual Gauge for Localized Orbitals (IGLO)[7-9] calculations of the shielding tensor with use of double-ζ basis sets. In the smaller molecules calculations with the addition of polarization functions to the basis sets were also performed.

II. Experimental Section

All spectra with the exception of ethane were taken at a temperature of about 25 K with an Air Products Displex 202-B refrigeration unit which has been described previously.[3] The samples were all deposited neat and were subjected to 4–5 freeze–pump–thaw cycles to remove dissolved oxygen. The sample of ethane was deposited neat on the sapphire rod of an Air Products Model No. LT-3-110 Heli-Tran and run at a temperature of about 7 K. All chemicals were obtained from standard commercial sources and used without further purification. Spectra were taken under the conditions reported previously.[1]

A new fitting procedure based on a simplex algorithm was used to vary the NMR parameters in the simultation of the experimental spectrum. The "best fit" spectrum is found when the sum of squares deviation between simulated and experimental spectra minus the sum of squares deviation of the spectrum forming the worst point in the "simplex" is less than some preset value (usually between 10^{-3} and 10^{-6}, with the highest point in the experimental spectrum set to unit intensity).

The NMR parameters that the simplex algorithm can vary are either the principal cartesian components (σ_{11}, σ_{22}, σ_{33}) or the irreducible spherical components (σ, δ, and η)[10] and a Lorentzian and Gaussian broadening function for each different ^{13}C shielding tensor in the molecule. The spherical set of parameters are defined as follows: $\sigma = 1/3(\sigma_{11} + \sigma_{22} + \sigma_{33})$, $\delta = \sigma_{33} - \sigma$, and $\eta = (\sigma_{11} - \sigma_{22})/\delta$. Any of the NMR parameters may be locked to any constant value during the fitting process as may be required by symmetry constraints imposed on the spin system. In the simulation of the ethane and neopentane spectra the irreducible set of shielding parameters was used with η locked to zero during the fitting process.

An error analysis is performed on the fit and the variance–covariance and correlation matrices of the fitting parameters are found. A marginal standard deviation of the fit parameters has been found to be less than or equal to 1 ppm for all fits in this paper. However, when the (σ_{11}, σ_{22}, σ_{33}) parametrization is used and two of the values (σ_{11} and σ_{22}) have a difference of about 1 ppm or less, the error analysis indicates a high correlation in these two parameters. If the spherical parametrization is then used the parameters σ and δ are well determined but η is not. This indicates that the average of two closely spaced shift values is well determined but that their difference is not. The errors in the fitting variables, which may be several marginal standard deviations in a multiparameter fit, are then equal to or less than the systematic errors, as large as 2–3 ppm, introduced from referencing to an external sample.

Since a large number of spectra must be calculated in the fitting procedure the new POWDER integration interpolation method[6] which greatly reduces computation time was used. The description of the fitting procedure is discussed elsewhere[6] in greater detail with the dimethoxymethane spectrum used as an example.

III. Quantum Chemical Calculations

Quantum chemical calculations of the shielding tensors of the molecules studied in this paper have been performed with the IGLO method.[7-9] All calculations used experimental geometries, except for dimethyl sulfite where the MNDO optimized geometry was employed (Appendix). Two Huzinaga basis sets[11] were used in the calculations. Basis set I is of double-ζ quality: (3) contracted to (2,1) in hydrogen, (7,3) contracted to (4111,21) for first-row atoms, and (9,5) contracted to (411111,2111) for the second-row atoms. For some smaller molecules calculations were performed with basis set II which included polarization functions. Basis set II is (5,1) contracted to (311,1) for hydrogen, (9,5,1) contracted to (51111,311,1) for first-row atoms, and (11,7,1) contracted to (5111111,31111,1) for second-row atoms. Exponents of 0.7, 1.0, 1.54, and 0.421 were used for the polarization functions in H, C, O, and S, respectively.

For comparison with experiment the calculated values were transformed to the Me_4Si scale as described previously,[1,2] using CH_4 absolute shielding values of 219 and 215 ppm respectively for basis sets I and II. The principal values reported here correspond to the symmetric part of the shielding tensor, as it is well documented that antisymmetric parts of the tensors do not contribute to the NMR spectrum to first order in the magnetic field.[12]

IV. Results and Discussion

The experimental and IGLO calculated chemical shielding principal values are shown in Table I along with their average and liquid values. The experimental values measured elsewhere, for CH_3F,[13] and *cis*- and *trans*-butene,[3] were included in Table I for comparison with IGLO calculations contained in this work. For the methyl groups in this study there was a consistent but modest downfield shift of about 2 ppm in going from the liquid to the solid state. This downfield shift, which may reflect referencing problems, seems to be more pronounced in methyls than in other groups.[1,2] The shielding in methyls can best be discussed by grouping them according to the atom to which they are bonded. In Table I they are classified as methoxy carbons and methyl carbons attached to carbon, to sulfur, or to fluorine.

Methoxy Methyls. There are six compounds listed in Table I which contain methoxy groups. Two of the compounds have multiple tensors listed: methanol, because of hydrogen bonding, and trimethoxymethane, because of conformational effects. The experimental shielding components for the methoxy tensors range from 3 ppm for the σ_{33} component in methanol to 98 ppm for σ_{11} in dimethoxymethane. The three principal values of the seven methoxy carbons (two for methanol) have averages (standard deviations) of σ_{11} = 81 (9) ppm, σ_{22} = 71 (8) ppm, and σ_{33} = 8 (3) ppm. These values are similar to those reported before for methoxy groups[14] but are slightly more downfield in σ_{11} and σ_{22}. The small standard deviation in the shifts of the σ_{33} component has also been found to be characteristic of the chemical shielding in methoxy groups.

The IGLO calculations for the methoxy tensors agree very well with the experimental values, but for the smaller molecules CH_3OH and CH_3OCH_3 there is a remarkable improvement in the calculated results when polarization functions are included in the basis set.

In trimethoxymethane the three methoxy groups are not equivalent if the solid sample has the same conformation that is most stable in the gas phase[15,16] from which it was deposited. In

(1) Facelli, J. C.; Orendt, A. M.; Beeler, A. J.; Solum, M. S.; Depke, G.; Malsch, K. D.; Downing, J. W.; Murthy, P. S.; Grant, D. M.; Michl, J. *J. Am. Chem. Soc.* **1985**, *107*, 6749.
(2) Facelli, J. C.; Orendt, A. M.; Solum, M. S.; Depke, G.; Grant, D. M.; Michl, J. *J. Am. Chem. Soc.* **1986**, *108*, 4268.
(3) Zilm, K. W.; Conlin, R. T.; Grant, D. M.; Michl, J. *J. Am. Chem. Soc.* **1980**, *102*, 6672.
(4) Beeler, A. J.; Orendt, A. M.; Grant, D. M.; Cutts, P. W.; Michl, J.; Zilm, K. W.; Downing, J. W.; Facelli, J. C.; Schindler, M. S.; Kutzelnigg, W. *J. Am. Chem. Soc.* **1984**, *106*, 7672.
(5) Orendt, A. M.; Facelli, J. C.; Grant, D. M.; Michl, J. M.; Walker, F. H.; Daily, F. H.; Waddel, S. T.; Wiberg, K. B.; Schindler, M.; Kutzelnigg, W. *Theor. Chim. Acta* **1985**, *68*, 421.
(6) Alderman, D. W.; Solum, M. S.; Grant, D. M. *J. Chem. Phys.* **1986**, *84*, 3717.
(7) Kutzelnigg, W. *Isr. J. Chem.* **1980**, *19*, 193.
(8) Schindler, M.; Kutzelnigg, W. *J. Am. Chem. Soc.* **1983**, *105*, 193.
(9) Schindler, M.; Kutzelnigg, W. *J. Chem. Phys.* **1982**, *76*, 1919.
(10) Haeberlen, U. In *High Resolution NMR in Solids*; Academic Press: New York, San Francisco, London, 1976; Adv. Magn. Reson., Volume Supplement 1.
(11) Huzinaga, S. *Approximate Atomic Wave Functions*; University of Alberta: Alberta, Edmonton, 1971.
(12) Griffin, R. G.; Ellet, J. D.; Mehring, M.; Bullitt, J. G.; Waugh, J. S. *J. Chem. Phys.* **1972**, *57*, 2147.
(13) Zilm, K. W.; Grant, D. M. *J. Am. Chem. Soc.* **1981**, *103*, 2913.
(14) Veeman, W. S. *Prog. NMR Spectrosc.* **1984**, *16*, 193.
(15) Spelbos, A.; Mijlhoff, F. C.; Faber, D. H. *J. Mol. Struct.* **1977**, *41*, 47.

Table I. Experimental and Calculated Principal Values of the ^{13}C Shielding Tensor for Methyl Carbons[a]

compd	σ_{11} exptl	σ_{11} calcd[b]	σ_{22} exptl	σ_{22} calcd[b]	σ_{33} exptl	σ_{33} calcd[b]	σ_{av} exptl	σ_{av} calcd[b]	σ_{liq}
CH_3OH[c]	76	64, 76	68	63, 71	6	6, 9	50	44, 52	49.0
acceptor	75	66	73	65	3	4	50	45	
donor	70	61	67	60	10	7	49	43	
CH_3OCH_3	88	78, 85	88	75, 81	6	4, 8	61	52, 58	59.7
$CH_3OCH_2OCH_3$	98	74	70	64	9	4	59	47	55.0
$(CH_3O)_3CH$[d]	80		65		11		52		51.1
1		66		60		7		44	
2		71		67		3		47	
3		75		64		5		48	
$(CH_3O)_4C$	78	65	71	61	9	3	52	43	50.0
$CH_3OS(O)OCH_3$	79	70	63	62	10	8	51	47	48.4
CH_3CH_3	11	9, 16	11	9, 16	4	−2, 5	9	5, 12	7.3
$CH_3CH_2CH_3$	30	24	15	17	4	−3	16	13	15.4
$(CH_3)_3CH$	42	36	33	29	6	−1	27	21	24.3
$(CH_3)_4C$	50	45	50	45	5	1	35	30	33.0
CH_3COCH_3[c]	49	45	47	40	−3	−6	31	26	29.8
CH_3CH_2OH[c]	35	36, 44	19	15, 21	4	−4, 2	19	16, 22	18.2
$(CH_3CH_2)_2O$[c]	32	33	15	17	9	−7	19	14	17.1
$HCH_3C{=}CCH_3H$									
cis[e]	28	33	6	15	6	7	13	18	12.1
trans[e]	27	32	27	29	5	0	20	20	17.6
CH_3F[f]	105	79, 97	105	79, 97	15	7, 9	75	55, 68	74.1
CH_3SH	14	24, 22	12	14, 19	2	−5, 0	9	11, 14	6.5
$(CH_3)_2S$	43	31	20	15	4	−11	22	12	18.2
CH_3SSCH_3	48	42	16	14	6	−6	23	17	22.1
$CH_3SO_2CH_3$	62	77	62	61	9	−14	44	41	42.8

[a] All experimental values in ppm referenced to Me_4Si, with the calculated values referenced to CH_4 as explained in the text. [b] The second shielding value was calculated with basis set II. [c] Other reported experimental values (σ_{11}, σ_{22}, σ_{33}) are the following: methanol (73, 73, 10); ethanol (24, 15, 0); diethyl ether (28, 18, 10); acetone (47, 47, −2); dimethyl disulfide (47, 17, 5) from ref 17 and methanol (74, 67, 3) from ref 18. [d] Values for the TGG conformer. The carbon nuclei are numbered as in ref 15. [e] Experimental shielding values from ref 3. [f] Experimental shielding values from ref 13.

a previous study[2] the shielding tensor of the central carbon was found not to be axially symmetric, indicating that the deposition process, at least to some extent, preserves the conformational equilibrium present in the gas phase. In the solid phase the compound assumes C_3 symmetry,[15,16] rendering the central carbon axially symmetric.

However, it was not possible to uniquely fit the experimental spectrum to three distinct tensors for the methoxy groups. The experimental values from the best single-tensor fit are reported in Table I. The IGLO calculations were performed with the gas phase conformation,[15,16] and the values for the three nonequivalent methoxy groups are reported in Table I.

The experimental spectrum of neat methanol at 25 K is shown in Figure 1a with the best-fit single-tensor spectrum superimposed. The fit is excellent except for the slope difference around the σ_{33} component. The tensor components from this fit are σ_{11} = 76 ppm, σ_{22} = 67 ppm, and σ_{33} = 6 ppm, which agree within experimental error with previously reported values.[17,18]

In the vapor phase, IR results show that methanol exists as monomers, open chain dimers, and cyclic tetramers,[19] while in the solid state both the α and β phases exist as long hydrogen bonded polymer chains.[20] In argon and nitrogen matrices a large variety of species from monomer to high polymer are present.[19]

To investigate the possibility that the deposited methanol sample may have quenched on the cyrotip with some vapor phase species present, rather than reordering to the solid state polymer structure, and showing different tensors for proton donors and acceptors, the experimental spectrum was refitted with two tensors (Figure 1b). This two-tensor fit shows considerable improvement over the single-tensor fit in the upfield σ_{33} region. The values from the two-tensor fit are σ_{11} = 70 ppm, σ_{22} = 67 ppm, and σ_{33} = 10 ppm for one tensor and σ_{11} = 75 ppm, σ_{22} = 73 ppm, and σ_{33} = 3 ppm for the other tensor.

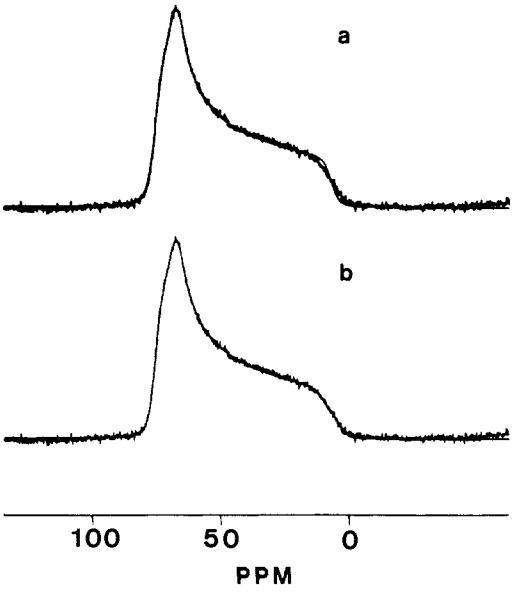

Figure 1. The experimental and best fit spectra of methanol. (a) The best-fit single-tensor spectrum superimposed on the experimental spectrum. (b) The best-fit two-tensor spectrum superimposed on the experimental spectrum.

IGLO calculations of the methanol monomer gave the components σ_{11} = 64 ppm, σ_{22} = 63 ppm, and σ_{33} = 6 ppm for both the staggered and eclipsed conformations with basis set I and the values σ_{11} = 76 ppm, σ_{22} = 71 ppm, and σ_{33} = 9 ppm in the staggered conformation with basis set II. Another calculation on an open-chain dimer[21] gave the tensor components σ_{11} = 61 ppm, σ_{22} = 60 ppm, and σ_{33} = 7 ppm for one tensor and the values σ_{11} = 66 ppm, σ_{22} = 65 ppm, and σ_{33} = 4 ppm for the other tensor. Therefore, in comparison to the monomer tensor, one tensor of

(16) Lee, H.; Wilnshurst, J. K. *Spectrochim. Acta* **1966**, *23*, 347.
(17) Pines, A.; Gibby, M. G.; Waugh, J. S. *Chem. Phys. Lett.* **1972**, *15*, 373.
(18) Matsui, S.; Terao, T.; Saika, A. *J. Chem. Phys.* **1982**, *77*, 1788.
(19) Barnes, A. J.; Hallam, H. E. *Faraday Soc. Trans.* **1970**, *66*, 1920.
(20) Tauer, K. J.; Lipscomb, W. N. *Acta Crystallogr.* **1952**, *5*, 606.
(21) Tse, Y. C.; Newton, M. D.; Allen, L. C. *Chem. Phys. Lett.* **1980**, *75*, 350.

the dimer has its anisotropy contracted while the anisotropy of the other tensor is expanded. These theoretical results arising from the hydrogen bonding are in qualitative agreement with the experimental results from the two-tensor fit. The errors of the present methods unfortunately approach the magnitudes of the proposed effects of aggregation, and a more extensive treatment of the matter must await improvements in both experimental and theoretical methods.

The σ_{11} = 98 ppm component in dimethoxymethane has the second farthest downfield component of methyl groups reported to date and is exceeded only by the perpendicular components in methyl fluoride.[13] This molecule also has the largest deviation from axial symmetry of the methoxy groups listed in Table I, showing a difference of 28 ppm between σ_{11} and σ_{22}. The IGLO calculations with basis set I and the nonplanar experimentally determined geometry[22] gave a difference of 10 ppm between these components. For an assumed trans planar geometry the calculated tensor was accidentally axially symmetric with the components: $\sigma_{11} = \sigma_{22}$ = 74 ppm and σ_{33} = 4 ppm. Calculations with a (51111,311) basis set give a difference between σ_{11} and σ_{22} of 16 ppm. Therefore calculations with a basis set without polarization functions were not capable of reproducing the 28 ppm shift difference between the two downfield components. This discrepancy is consistent with the result in methyl fluoride where the calculations fail to reproduce the experimental values of the perpendicular components without polarization functions. Likewise, in dimethyl ether the use of polarization functions improves significantly the values in the downfield components.

Methyl Groups Bonded to Carbon Atoms. There are seven compounds in Table I which have the methyl group attached to a carbon atom, not including the two butenes whose experimental values were reported previously.[3] The averages (standard deviation) of the three shielding tensor components are σ_{11} = 36 (13) ppm, σ_{22} = 27 (16) ppm, and σ_{33} = 4 (4) ppm. These are very similar to previously reported values.[14] Three of the compounds, acetone, ethanol, and diethyl ether, have had somewhat similar values reported at higher temperatures.[17]

As observed in methoxy groups, the σ_{33} component is very constant from compound to compound. On the average, it is about 5-ppm downfield in methoxy groups compared to methyls attached to carbon atoms. In methoxy groups the σ_{11} and σ_{22} components are close together, while σ_{33} is well separated from them. For the methyls attached to carbons a much narrower spread in the tensor components is observed than for the methoxy groups, indicating the importance of electronegative substituents for the shift of the two perpendicular components.

For methyls attached to carbon there is excellent agreement between the experimental shielding components and the IGLO values. Agreement is within 11 ppm for all but the σ_{33} component in diethyl ether. The value of this σ_{33} component may be improved with use of basis set II as was the case in ethane and ethanol.

Methyls Attached to Sulfur Atoms. For the three compounds in Table I in which the methyl group is next to a sulfur atom, not including dimethyl sulfone which also shows effects from oxygen, the averages (standard deviations) of the three tensor components are σ_{11} = 35 (18) ppm, σ_{22} = 16 (4) ppm, and σ_{33} = 4 (2) ppm. There is also a small variation in the values of the σ_{33} component in this class of methyls, as is seen in other methyl groups. Almost identical values for the shielding components of dimethyl disulfide, at a somewhat higher temperature, have been previously reported.[17]

There is reasonably good agreement between the experimental and the IGLO shielding components in the four sulfur compounds. The agreement is not quite as good as with other types of methyls, especially in the σ_{33} component where the calculated values are 7–15-ppm upfield. In methanethiol there is an improvement in this component when polarization functions are added to the basis set, but the paramagnetic contributions in the other two components seem to be overestimated.

IGLO calculations do not reproduce the experimental shielding components for dimethyl sulfone. The calculated σ_{33} component is 23-ppm upfield of the experimental value, and the calculations predict a difference of 16 ppm between σ_{11} and σ_{22}, which experimentally are found to be accidentally degenerate.

(22) Astrup, E. E. *Acta Chem. Scand.* **1973**, *27*, 3271.

Table II. Calculated Angles between σ_{33} and the C_3 Symmetry Axis of the Methyl Group

compound	angle[a] (deg)	compound	angle[a] (deg)
CH_3OH	0.3[b] (0.8)	CH_3COCH_3	8.0
CH_3OCH_3	2.9 (1.3)	CH_3CH_2OH	15.2 (14.0)
$CH_3OCH_2OCH_3$	2.8	$(CH_3CH_2)_2O$	9.5
$CH_3OS(O)OCH_3$	2.9		
		CH_3SH	1.1 (8.3)
$(CH_3)_3CH$	7.3	$(CH_3)_2S$	5.0
$CH_3CH_2CH_3$	11.8	CH_3SSCH_3	9.1
$HCH_3C{=}CCH_3H$		$CH_3SO_2CH_3$	0.4[c]
cis	1.8		
trans	0.7		

[a] Values in parentheses calculated with basis set II. [b] 2.7 in the eclipsed conformation, using basis set I. [c] An experimental value of 2.5 reported before in ref 23.

V. Orientation of the Shielding Tensor in Methyl Groups

The orientation of the methyl shielding tensor has been determined experimentally in a few compounds, by either symmetry, single-crystal studies,[14] motional studies, [23] or dipolar spectroscopy.[14] For the compounds studied here the experimental technique used precludes the experimental assignment of the shielding tensor components into the molecular frame, except in those cases where the molecule has at least a C_3 axis through the CH_3 carbon. This is the case in CH_3F, $(CH_3)_4C$, and CH_3CH_3, and σ_{33} lies along the C–X bond. In each instance the IGLO results agree with these assignments.

Most of the molecules in Table I exhibit two close components downfield and one component upfield. As discussed above, this σ_{33} component is almost independent of the substituent attached to the methyl group. In all cases the theory places σ_{33} along or nearly along the C–X bond. The calculated angles of deviation from the bond direction are given in Table II.

These calculations confirm the explanation suggested[3] for the anomalous shielding tensors in *cis*- and *trans*-butene. In these two compounds a unique component is σ_{11} in the cis compound and σ_{33} in *trans*-butene. The IGLO calculations show in both cases that σ_{33} is the component aligned in the general direction of the C–C bond while σ_{22} is accidentally degenerate with σ_{11} in *trans*-butene and with σ_{33} in *cis*-butene. Conformational crowding is probably responsible for these anomalous shifts.[24]

In Figure 2 the experimental principal shielding values in *cis*- and *trans*-butene have been placed in the molecular frame[25,26] in accordance with the assignment given by the IGLO calculations. The results in Figure 2 clearly show that the two in-plane (C=C—CH_3) components are essentially the same for both molecules. The component perpendicular to the plane moves 21 ppm upfield in the cis compound relative to the trans one.

In the compounds in which σ_{11} and σ_{22} are not degenerate the IGLO calculations give an approximate tensor orientation. The component σ_{11} is either perpendicular or approximately perpendicular, depending on symmetry, to the H_3–C–X–Y plane in dimethyl ether, *trans*-2-butene, dimethyl sulfide, methanethiol, dimethoxymethane, diethyl ether, ethanol, and dimethyl disulfide, whereas σ_{22} is the component perpendicular to the H_3–C–X–Y plane in methanol, dimethyl sulfite, propane, isobutane, acetone, *cis*-2-butene and dimethyl sulfone. In the cases for which calculations were also performed with basis set II, this assignment remained unchanged. In methanol these assignments are also independent of the conformation used in the calculations, whether staggered or eclipsed.

(23) Solum, M. S.; Zilm, K. W.; Michl, J.; Grant, D. M. *J. Phys. Chem.* **1983**, *87*, 2940.
(24) Li, S.; Chesnut, B. *Magn. Reson. Chem.* **1985**, *23*, 625.
(25) Kondo, S.; Sakurai, Y.; Hirota, E.; Morino, Y. *J. Mol. Spectrosc.* **1970**, *34*, 231.
(26) Almenningen, A.; Anfinsen, I. M.; Haaland, A. *Acta Chem. Scand.* **1970**, *24*, 43.

Table III. IGLO Bond Contributions, $\sigma_{\mu\lambda}^{CX}$, to the ^{13}C Shielding Tensor in the Local Bond Frames for Methyl Groups[a]

compd	$\sigma_{\mu\lambda}^{CH_1}$ [b]			$\sigma_{\mu\lambda}^{CH_{2,3}}$ [b]			$\sigma_{\mu\lambda}^{CX}$ [c]		
CH_3CH_3	0.00	1.26	0	0.00	1.26	0	0.00	0	0
	1.26	−14.34	0	1.26	−14.34	0	0	−14.91	0
	0	0	−12.85	0	0	−12.85	0	0	−14.91
CH_3F	0.10	0.59	0	0.10	0.59	0	0.00	0	0
	0.59	−16.91	0	0.59	−16.91	0	0	−20.02	0
	0	0	−51.31	0	0	−51.31	0	0	−20.02
CH_3OH	0.07	2.19	0	0.04	1.51	∓0.99	0.02	−0.37	0
	2.19	−16.98	0	1.51	−16.90	±2.13	−0.37	−24.15	0
	0	0	−39.12	∓0.99	±2.13	−39.60	0	0	−18.8
CH_3OCH_3	0.07	−0.70	0	0.06	−1.55	∓1.02	−0.04	1.17	0
	−0.70	−18.83	0	−1.55	−16.92	±0.32	1.17	−30.23	0
	0	0	−46.72	∓1.02	±0.32	−40.79	0	0	−24.04
CH_3SH	0.03	−0.61	0	0.05	−0.98	∓1.21	0.01	−0.38	0
	−0.61	−12.95	0	−0.98	−13.19	±0.16	−0.38	−12.88	0
	0	0	−26.65	∓1.21	±0.16	−18.27	0	0	−9.31
CH_3SCH_3	0.02	−0.13	0	0.04	−0.86	±1.66	−0.01	0.39	0
	−0.13	−10.68	0	−0.86	−12.09	±0.98	0.39	−12.60	0
	0	0	−29.53	±1.66	±0.98	−20.41	0	0	−11.05
$CH_3CH_2CH_3$	0.05	−1.19	0	0.06	−1.22	±0.54	−0.01	1.17	0
	−1.19	−15.56	0	−1.22	−14.72	±0.72	1.17	−18.98	0
	0	0	−16.90	±0.54	±0.72	−14.41	0	0	−20.21
CH_3CH_2OH	−0.02	1.17	0	0.03	1.29	∓1.45	0.00	−1.61	0
	1.17	−14.23	0	1.29	−13.30	±0.82	−1.61	−17.10	0
	0	0	−23.82	∓1.45	±0.82	−16.17	0	0	−22.79

[a] All values in ppm. Only the paramagnetic contributions calculated with basis set I are shown. $\mu, \lambda = i, j, k$. i: along the C–X or H–C bond. j: perpendicular to the C–X or H–C bond in the H–C–X plane. k: perpendicular to i and j. (See Figure 2.) Note that the bond contributions, which are given in different frames, have to be rotated to the molecular frame, in which they can be added to obtain the total shielding tensor. [b] The $C-H_1$ bond is contained in the H–C–X symmetry plane, while $C-H_{2,3}$ are the bonds placed as mirror images relative to the symmetry plane of the molecule. The ± sign is required by the symmetry of total shielding tensor as explained in the text. [c] X = C, O, S, or F.

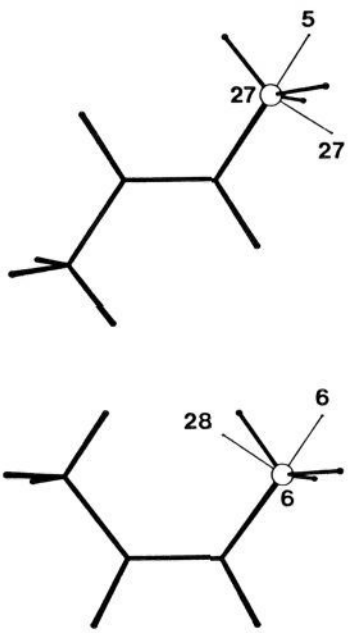

Figure 2. The experimental principal shielding tensor components placed in the molecular frame according to the IGLO results in *cis*- and *trans*-butene. There is one component perpendicular to the plane of the paper in each molecule.

VI. IGLO Bond Contributions

Recent work[27] has shown that a valuable insight into the origin of chemical shielding can be obtained by analyzing the IGLO bond contributions in the local bond frame. For that purpose the IGLO bond contributions, $\sigma_{\mu\lambda}^{XY}$, from a X–Y bond can be rotated to the local bond frame defined by an axis, i, along the X–Y bond, and two perpendicular axes j and k. If the molecule has a symmetry plane passing through the C–X bond, j is chosen to lie in it and k perpendicular to it. In the absence of a symmetry plane a third atom, Z, different from hydrogen if possible, is chosen to determine the plane in which i and j lie. Again k is selected perpendicular to the plane (see Figure 3).

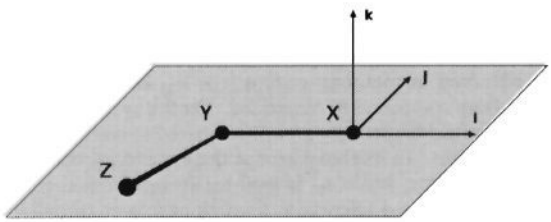

Figure 3. Description of the local bond axis system.

In Table III the bond contributions in the local bond frame for the C–X (X = O, F, C, or S), $C-H_1$, and $C-H_{2,3}$ bonds are given for representative compounds. As the compounds listed in Table III exhibit a symmetry plane, there are then two kinds of C–H bonds. The bond contributions from the $C-H_1$ bonds, those in the symmetry plane, exhibit the same symmetry properties as those contributions of the C–X bonds, i.e., $\sigma_{\mu k}^{CH} = 0$ for $\mu = i, j$. For the contributions of the other two C–H bonds ($C-H_{2,3}$) the symmetry requirements are absent, but the overall molecular symmetry requirement on the shielding tensor introduces a change of sign in $\sigma_{ik}^{CH'}$ and $\sigma_{jk}^{CH'}$ from one bond to its mirror image, which when summed together always cancel one another thereby preserving the C_2 symmetry features in the overall shielding tensor.

All C–H and C–X bond contributions show either zero or almost negligible contributions for the component along the bond. This theoretical result indicates that the electronic distribution has cylindrical symmetry along the C–X bonds in support of classical concepts of a chemical bond. Different results have been found to be characteristic of strained bonds.[27]

(27) Facelli, J. C.; Grant, D. M.; Michl, J. *Int. J. Quantum Chem.*, Proceedings of the 1986 Sanibel Symposium, in press.

Table IV. IGLO Bond Contributions to the ^{13}C Shielding Tensor in the Local Bond Coordinate System for *cis*- and *trans*-Butene[a,b]

compd	$\sigma^{CC}_{\mu\lambda}$			$\sigma^{CH_1}_{\mu\lambda}$			$\sigma^{CH_{2,3}}_{\mu\lambda}$		
cis	0.00	−0.11	0	−0.02	2.36	0	0.01	0.94	∓0.64
	−0.11	−23.75	0	2.36	−17.43	0	0.94	−14.22	∓0.13
	0	0	−15.44	0	0	−16.33	∓0.64	∓0.13	−18.90
trans	−0.01	−0.01	0	0.23	−1.23	0	−0.06	−2.22	∓0.75
	−0.01	−22.98	0	−1.23	−16.05	0	−2.22	−13.02	∓0.98
	0	0	−22.54	0	0	−19.44	∓0.75	∓0.98	−18.51

[a] All values in ppm. Only the paramagnetic contributions calculated with basis set I are shown. $C-H_1$ is in the symmetry plane; $C-H_2$ and $C-H_3$ lie as mirror images with respect to the plane. $\mu, \lambda = i, j, k$. [b] *i*: along the C-C or H-C bond. *j*: perpendicular to the C-C or H-C bond in the H-C-C plane. *k*: perpendicular to *i* and *j*. (See Figure 2.)

It is interesting that direct C-X bond contributions to the overall substituent effects are relatively modest and that the C-H bonds adjacent to the C-X bonds contribute significantly to the overall substituent shifts. From the results in Table III it is clear that a sizable contribution to the substituent shift in the ^{13}C shielding tensor comes from σ^{CH}_{kk}. This sensitivity of σ^{CH}_{kk} on the substituent can be rationalized in terms of the orbital mixing of the occupied C-H orbital with the C-X antibonding orbital.

The data in Table III can be used to explain the relative invariance of σ_{33} along the series of compounds in this study. If trigonal symmetry is assumed, then the IGLO bond contributions, in the local frame, are related to the principal shielding tensor components by

$$\sigma_{\parallel} = 3[\sigma^{CH}_{ii} \cos^2\theta + 2\sigma^{CH}_{ij} \cos\theta \sin\theta + \sigma^{CH}_{jj} \sin^2\theta] \quad (1)$$

$$\sigma_{\perp} = (3/2)[\sigma^{CH}_{jj} \cos^2\theta - 2\sigma^{CH}_{ij} \cos\theta \sin\theta + \sigma^{CH}_{ii} \sin^2\theta + \sigma^{CH}_{kk}] + 1/2[\sigma^{CX}_{jj} + \sigma^{CX}_{kk}] \quad (2)$$

where θ is the HCX angle and only directly attached bonds are considered. From eq 1 and 2 it is apparent that $\sigma_{\parallel}$ does not depend on σ^{CH}_{kk}, which is the bond contribution that carries most of the substituent effect. The other contributions to $\sigma_{\parallel}$ are almost substituent independent as discussed.

When trigonal symmetry is absent but a symmetry plane is present the non-zero components of the shielding tensor are given by

$$\sigma_{\alpha\alpha} = \sigma^{CH}_{ii} \cos^2\theta + 2\sigma^{CH'}_{ii} \cos^2\theta + 2\sigma^{CH}_{ij} \cos\theta \sin\theta + 4\sigma^{CH'}_{ij} \cos\theta \sin\theta + \sigma^{CH}_{jj} \sin^2\theta + 2\sigma^{CH'}_{jj} \sin^2\theta + \sigma^{CX}_{ii} \quad (3)$$

$$\sigma_{\beta\beta} = -(3)^{1/2}\sigma^{CH'}_{jk} \cos\theta + (3)^{1/2}\sigma^{CH'}_{ki} \sin\theta + \sigma^{CH}_{jj} \cos^2\theta + (1/2)\sigma^{CH'}_{jj} \cos^2\theta - 2\sigma^{CH}_{ij} \cos\theta \sin\theta - \sigma^{CH'}_{ij} \cos\theta \sin\theta + \sigma^{CH}_{ii} \sin^2\theta + 2\sigma^{CH'}_{ii} \sin^2\theta + (3/2)\sigma^{CH'}_{kk} + \sigma^{CX}_{jj} \quad (4)$$

$$\sigma_{\alpha\beta} = (3)^{1/2}\sigma^{CH'}_{ik} \cos\theta + (3)^{1/2}\sigma^{CH'}_{jk} \sin\theta + (\sigma^{CH}_{ij} - \sigma^{CH'}_{ij}) \times (\cos^2\theta - \sin^2\theta) + (\sigma^{CH}_{jj} - \sigma^{CH'}_{jj} + \sigma^{CH'}_{ii} - \sigma^{CH}_{ii}) \cos\theta \sin\theta \quad (5)$$

$$\sigma_{\gamma\gamma} = (3)^{1/2}\sigma^{CH'}_{jk} \cos\theta - (3)^{1/2}\sigma^{CH'}_{ki} \sin\theta + 3/2\sigma^{CH'}_{jj} \cos^2\theta - 3\sigma^{CH'}_{ij} \cos\theta \sin\theta + 3/2\sigma^{CH'}_{ii} \sin^2\theta + \sigma^{CH}_{kk} + 1/2\sigma^{CH'}_{kk} + \sigma^{CX}_{kk} \quad (6)$$

where α is the direction along the methyl top axis, γ is perpendicular to the symmetry plane, and β is perpendicular to α in the symmetry plane. Also, in the above equations $\sigma^{CH'}_{\mu\lambda}$ represents the magnitude of the bond contributions from the $C-H_{2,3}$ bonds. The change of sign in the off-diagonal terms of the $C-H_{2,3}$ bond contribution has been taken into account explicitly in eq 3-6. $\sigma^{CH}_{\mu\lambda}$ are the contributions from the C-H bond in the symmetry plane. In this case $\sigma_{\mu\gamma}$ for $\mu = \alpha, \beta$ are identically 0 by symmetry. As in the case of trigonal symmetry, the component along the bond, $\sigma_{\alpha\alpha}$, is independent of σ^{CH}_{kk}. As a consequence theory predicts that $\sigma_{\alpha\alpha}$ is almost substituent independent as has been found experimentally.

The asymmetry, η, in the shielding tensor can originate from two different sources, either a nonaxial contribution from the C-X bond and/or a difference in the contributions from the $C-H_1$ and $C-H_{2,3}$ bonds (eq 3-6). The results in Table III show that the contributions to the asymmetry of the shielding tensor from the C-X bonds are less than 7 ppm. It is also clear that the large asymmetries observed in CH_3SH and CH_3SCH_3 originate in the differences between the contributions of the two types of C-H bonds as is shown in Table III. In cases in which the asymmetry of the shielding tensor is modest, it is not always possible to attribute the effect to a dominant term. In such cases the origin of the asymmetry is not readily recognized because of the complexity of eq 3-6.

In Table IV the IGLO bond contributions to the methyl shielding tensor in *cis*- and *trans*-butene are displayed. It is observed that the largest contribution to the upfield shift observed in the cis compound arises from the C-C bond (7 ppm). Significant contributions are also observed from the C-H bonds. The $C-H_1$ bond contributes 3 ppm while the $C-H_{2,3}$ bonds contribute 1 ppm each. Note that the 2-ppm contribution from both $C-H_{2,3}$ bonds is not evident from the results in Table IV but can be obtained by rotating the bond contributions back into the molecular frame. In the trans compound the remote contributions are somewhat larger than in the cis compound, and that accounts for the final differences between the two compounds.

VII. Conclusions

This work shows that quantum chemical calculations are very useful not only in making tentative assignments of tensor components but also in the analysis of the relationship between the shielding tensor components and molecular structure. The almost constant value of the σ_{33} component from molecule to molecule can be understood in terms of IGLO bond contributions. Also, the sources of the anisotropy and asymmetry of the methyl tensor are explained well in terms of IGLO bond contributions. This indicates that the shielding properties of $^{13}CH_3$ groups are not related to the rotation of the methyls, which is not included in the quantum mechanical calculations.

This study also shows that the addition of polarization functions to the basis set generally improves the calculation of the σ_{33} component in all types of methyl groups but that they are especially important in calculating the perpendicular components when the methyl group is next to an electronegative atom such as oxygen or fluorine. Similar results on the importance of polarization functions in the calculation of isotropic shielding have been reported in the literature.[28]

Appendix

IGLO shielding calculations in dimethyl sulfite were performed with the MNDO optimized geometry. The MNDO[29] method was used without modifications for the geometry optimization. The optimization was done over all bond angles, bond lengths, and dihedral angles, but keeping the C_2 symmetry of the molecule. The optimized parameters are $r_{S=O}$ = 1.4835 Å, r_{S-O} = 1.6292 Å, r_{C-O} = 1.3937 Å, r_{C-H} = 1.1168 Å for the bond lengths, OSO = 105.96°, SOC = 128.91°, OCH = 110.58° for the bond angles, and OSOO = 105.52° and COCO = 0.11° for the dihedral angles.

Acknowledgment. This work was supported by the National Science Foundation under Grant CHE 83-10109. The authors are grateful to Drs. W. Kutzelnigg and M. Schindler for a copy of their IGLO program and the calculations in $(CH_3O)_4C$ and

(28) Ditchfield, R. *J. Chem. Phys.* **1981**, *63*, 185.
(29) Dewar, M. J. S.; Thiel, W. *J. Am. Chem. Soc.* **1977**, *99*, 4899.

$(CH_3O)_2CH_2$ and to Dr. J. W. Downing for adapting the IGLO program.

Registry No. CH_3OH, 67-56-1; CH_3OCH_3, 115-10-6; $CH_3OCH_2OCH_3$, 109-87-5; $(CH_3O)_3CH$, 149-73-5; $(CH_3O)_4C$, 1850-14-2; $CH_3OS(O)OCH_3$, 616-42-2; CH_3CH_3, 74-84-0; $CH_3CH_2CH_3$, 74-98-6; $(CH_3)_3CH$, 75-28-5; $(CH_3)_4C$, 463-82-1; CH_3COCH_3, 67-64-1; CH_3CH_2OH, 64-17-5; $(CH_3CH_2)_2O$, 60-29-7; *cis*-$HCH_3C{=}CCH_3H$, 590-18-1; *trans*-$HCH_3C{=}CCH_3H$, 624-64-6; CH_3F, 593-53-3; CH_3SH, 74-93-1; $(CH_3)_2S$, 75-18-3; CH_3SSCH_3, 624-92-0; $CH_3SO_2CH_3$, 67-71-0.

Ultraviolet Resonance Raman Spectroscopy of Imidazole, Histidine, and Cu(imidazole)$_4^{2+}$: Implications for Protein Studies

Debra S. Caswell and Thomas G. Spiro*

Contribution from the Department of Chemistry, Princeton University, Princeton, New Jersey 08544. *Received February 6, 1986*

Abstract: Raman spectra have been obtained for aqueous imidazole, imidazolium, 4-methylimidazole, histidine, histidinium, and Cu(imidazole)$_4^{2+}$, with ultraviolet excitation at wavelengths from 229 to 200 nm provided by a H_2-Raman-shifted Nd:YAG laser. In every case, the excitation profiles show maxima at ~218 and ~204 nm, within the broad ~210-nm electronic absorption band. The two maxima are identified with the first two $\pi-\pi^*$ transitions of the imidazole ring on the basis of the ring mode enhancement patterns. Substantial alterations of Raman-band frequencies and intensities are observed when the imidazole is protonated and/or substituted with a methyl group. The 4-methylimidazole spectra are similar to those of histidine. Coordination of Cu^{2+} to the imidazole has a smaller effect; several ring modes shift by a few wavenumbers. The imidazole(n) → Cu^{2+} charge-transfer transition is assigned near 240 nm on the basis of a Cu–N stretching mode enhancement similar to that of Cu(ethylenediamine)$_2^{2+}$ which has its charge-transfer band at this wavelength. Specific enhancement of a 950-cm^{-1} ring mode is also observed at 240 nm. Attempts to obtain RR spectra in the region (~300 nm) of the very weak imidazole(π) → Cu^{2+} charge-transfer transitions were unsuccessful. Although differences in the band positions might be used to distinguish protonated, unprotonated, and Cu-bound histidine residues in proteins, the overall enhancement is modest, and histidine signals are difficult to detect in the presence of the much larger signals from aromatic residues that are present in most proteins, as is illustrated in the case of the Cu protein stellacyanin.

It has recently become possible to obtain Raman spectra of biological molecules with excitation in the deep ultraviolet region via a pulsed Nd:YAG laser equipped with nonlinear optical frequency shifting devices.[1-3] Large resonance enhancements are seen for aromatic chromophores, such as the purine and pyrimidine bases of nucleic acids[4,5] and the phenylalanine, tyrosine, and tryptophan side chains of proteins,[6-8] as well as for the amide bands of the polypeptide chain.[6b,9] The imidazole ring of histidine also has $\pi-\pi^*$ transitions in the deep UV and is a candidate for UV resonance enhancement. Histidine side chains of proteins play important roles as acid–base catalysts, and as ligands to protein-bound metal ions. It would therefore be of considerable interest to characterize the chemical environments of histidine using ultraviolet resonance Raman (UVRR) spectroscopy.

In this study we explore resonance effects in the deep UV (229–200 nm) Raman spectra of imidazole (ImH) and the imidazolium ion (ImH_2^+), of the Cu(ImH)$_4^{2+}$ complex, and of histidine (HisH), histidinium ($HisH_2^+$), and 4-methylimidazole (4-MeImH). Resonance enhancement of the imidazole ring modes is seen in each case, the intensity pattern varying with the excitation wavelength. Excitation profiles (EP's) in the 229–200-nm region show two distinct maxima, at ~218 and ~204 nm, for each of these molecules, although only a single broad absorption band peaking at ~207 nm is observed in solution. These EP maxima are identified with the first two imidazole $\pi-\pi^*$ electronic transitions, on the basis of previously reported calculations;[10] the changes in the relative intensities of individual ring modes are consistent with these assignments. The data lend no support for assigning the ImH(n) → Cu charge-transfer (CT) transition at ~220 nm as previously proposed.[11] This transition is reassigned to an absorption shoulder at ~240 nm, similar in strength and wavelength to the CT band of Cu(en)$_2^{2+}$. RR spectra with 240-nm excitation show similar enhancements of the Cu–N breathing modes in the two complexes. Specific enhancement of a ImH ring mode, at 950 cm^{-1}, is also noted at this wavelength. Attempts to obtain Raman spectra in resonance with the very weak (ϵ ~ 300 M^{-1} cm^{-1}) ImH(π) → Cu CT transitions near 300 nm[11] were unsuccessful, the enhancement being too low.

Marked changes are seen in the vibrational frequencies among the imidazole derivatives. Although the Raman signature of the

(1) Ziegler, L. D.; Hudson, B. *J. Chem. Phys.* **1981**, *74*, 982.
(2) Asher, S. A.; Johnson, C. R.; Murtaugh, J. *Rev. Sci. Instrum.* **1983**, *54*, 1657.
(3) Fodor, S. P. A.; Rava, R. P.; Copeland, R. A.; Spiro, T. G. *J. Raman. Spectrosc.*, in press.
(4) (a) Ziegler, L. D.; Hudson, B.; Strommen, D. P.; Peticolas, W. L. *Biopolymers* **1984**, *23*, 2067. (b) Kubasek, W. L.; Hudson, B.; Peticolas, W. L. *Proc. Natl. Acad. Sci. U.S.A.* **1985**, *64*, 451.
(5) (a) Fodor, S. P. A.; Rava, R. P.; Hays, T. R.; Spiro, T. G. *J. Am. Chem. Soc.* **1985**, *107*, 1520. (b) Fodor, S. P. A.; Spiro, T. G. *Ibid.* **1986**, *108*, 3198.
(6) (a) Rava, R. P.; Spiro, T. G. *J. Am. Chem. Soc.* **1984**, *106*, 4062. (b) Rava, R. P.; Spiro, T. G. *Biochemistry* **1985**, *24*, 1861.
(7) Rava, R. P.; Spiro, T. G. *J. Phys. Chem.* **1985**, *89*, 1856.
(8) Johnson, C. R.; Ludwig, M.; O'Donnell, S.; Asher, S. A. *J. Am. Chem. Soc.* **1984**, *106*, 5008.
(9) (a) Copeland, R. A.; Spiro, T. G. *Biochemistry* **1985**, *24*, 4960. (b) Copeland, R. A.; Spiro, T. G. *J. Am. Chem. Soc.* **1986**, *108*, 1281.
(10) Bernarducci, E.; Bharadwaj, P. K.; Krogh-Jespersen, K.; Potenza, J. A.; Schugar, H. J. *J. Am. Chem. Soc.* **1983**, *105*, 3860.
(11) Fawcett, T. G.; Bernarducci, E. E.; Krogh-Jespersen, K.; Schugar, H. J. *J. Am. Chem. Soc.* **1980**, *102*, 2598.

0002-7863/86/1508-6470$01.50/0